Biomaterials Science

PAPER

View Article Online
View Journal | View Issue

Cite this: *Biomater. Sci.*, 2017, **5**, 784

Development of kartogenin-conjugated chitosan–hyaluronic acid hydrogel for nucleus pulposus regeneration

Yanxia Zhu,*[a] Jie Tan,[b] Hongxia Zhu,[c] Guangyao Lin,[a] Fei Yin,[a] Liang Wang,[a] Kedong Song,[d] Yiwei Wang,[e] Guangqian Zhou[a] and Weihong Yi*[b]

Injectable constructs for *in vivo* gelation have many advantages in the regeneration of degenerated nucleus pulposus. In this study, an injectable hydrogel consisting of chitosan (CS) and hyaluronic acid (HA) crosslinked with glycerol phosphate (GP) at different proportions (CS : GP : HA, 6 : 3 : 1, 5 : 3 : 2, 4 : 3 : 3, 3 : 3 : 4, 2 : 3 : 5, 1 : 3 : 6, V : V : V) was developed and employed as a delivery system for kartogenin (KGN), a biocompound that can activate chondrocytes. *In vitro* gelation time, morphologies, swelling, weight loss, compressive modulus and cumulative release of KGN in hydrogels were studied. For biocompatibility assessments, human adipose-derived stem cells (ADSCs) were encapsulated in these hydrogels. The effects of KGN on stem cell proliferation and differentiation into nucleus pulposus-like cells were examined. The hydrogels with higher concentrations of HA showed a slightly shorter gelation time, higher water uptake, faster weight loss and faster KGN release compared to the hydrogels with lower concentrations of HA. As the KGN-conjugated hydrogel prepared with the proportions 5 : 3 : 2 displayed good mechanical properties, it was chosen as the optimal gel to promote cell proliferation and differentiation. No significant difference was seen in the expression levels of nucleus pulposus markers induced by KGN or TGF-β. Additionally, inclusion of KGN and TGF-β together did not produce a synergistic effect in inducing nucleus pulposus properties. In conclusion, we have developed a KGN-conjugated CS/HA hydrogel (5 : 3 : 2) with sustained release of KGN in hydrogel that can promote ADSC proliferation and nucleus pulposus differentiation. This kind of hydrogel may be a simple and effective candidate for the repair of degenerative NP tissue after minimally invasive surgery.

Received 1st January 2017,
Accepted 20th February 2017

DOI: 10.1039/c7bm00001d

rsc.li/biomaterials-science

Introduction

Degenerative disc disease is the main cause of chronic low back pain and disability in the elderly. As discs degenerate, there is a decrease in the water content and a reduction in type II collagen and proteoglycans in the nucleus pulposus (NP), resulting in structural destruction and flattening of the disc.[1,2] Conventional approaches such as conservative treatment and surgical techniques can relieve the patients' clinical symptoms to some extent.[2,3] However, interest in developing biomaterials to regenerate the NP is growing dramatically, as biomaterials (with or without graft cells) provide a new strategy for restoring native tissue structures and the mechanical function. When the diseased NP tissue has been surgically removed, scaffolds constructed with biomaterials can be used for cell- and factor-delivery, which is aimed at tissue regeneration and finally, rehabilitation of normal disc function.

Although *in vitro* cell based engineered tissue has shown promising results in clinical studies, there are some limitations in clinical application, such as invasive surgery, inflammation, and subsequent infection. Injectable *in situ*-forming hydrogels can thus overcome these limitations, as they merely involve delivery *via* syringe injection during minimally invasive surgery, introducing the aqueous solution into the body at target sites to fill irregularly shaped defects.[4,5] *In situ*-forming hydrogels are particularly suitable for disc transplantation

[a]*Shenzhen Key Laboratory for Anti-ageing and Regenerative Medicine, Health Science Center, Shenzhen University, Shenzhen 518060, China. E-mail: yanxiazhu@szu.edu.cn; Fax: +86-755-86671906; Tel: +86-755-86671903*
[b]*Department of Spinal Surgery, Shenzhen Sixth People's Hospital (Nanshan Hospital), Shenzhen, 518060, China. E-mail: szyiwh@163.com; Fax: +86-755-86671906; Tel: +86-755-86671903*
[c]*Department of Spinal Surgery, Xiaogan Maternity&Child Healthcare Hospital, Xiaogan, 432100, China*
[d]*State Key Laboratory of Fine Chemicals, Dalian R&D Center for Stem Cell and Tissue Engineering, Dalian University of Technology, Dalian 116024, China*
[e]*Burns Research Group, ANZAC Research Institute, University of Sydney, Concord, NSW, 2139, Australia*

because of their cavity structures, and have become increasingly attractive in NP and cartilage tissue engineering[6,7] as well as drug delivery.[8]

Scaffold materials for cell- and factor-delivery should be biomimetic and should contain components of the extracellular matrix (ECM) in order to illicit specific cellular responses and direct new tissue formation.[9] Among various biomaterials, sodium hyaluronate/hyaluronic acid (HA) is a natural, biocompatible and biodegradable polysaccharide.[10] Moreover, it is a major component of synovial fluid as well as glycosaminoglycans (GAGs) that are found in the NP and articular cartilage. HA has been used broadly for osteoarthritis treatment,[11] as an intra-articular injective material, and has been proven to support cell proliferation and maintain the chondrogenic phenotype.[12] It has been demonstrated that HA-based hydrogels can direct recovery or replacement of the endogenous NP for NP tissue engineering and cellular therapies.[13] Another suitable candidate for cartilage and NP tissue repair is chitosan. Chitosan is structurally analogous to GAGs,[14] and is also non-toxic, water soluble, biodegradable, biocompatible and displays anti-bacterial properties. Chitosan has been investigated extensively for drug delivery systems.[15] The chitosan–gelatin scaffold prepared by the freeze-gelation method provides better conditions for NP cell proliferation.[16] The advantage of ECM molecules is that it allows cells to maintain their differentiated phenotype for specific tissues.

In addition to the material in the scaffold, growth factors are also important for tissue regeneration. The small molecule KGN can promote the selective differentiation of mesenchymal stem cells (MSCs) into chondrocytes, and has been identified as a chondrogenic and chondroprotective agent.[17,18] In a mouse model of osteoarthritis, intra-articular injection of KGN has been demonstrated to reduce tibial plateau cartilage degeneration.[19] Accordingly, KGN is expected to be a potential novel therapeutic drug for the treatment of osteoarthritis.

In this study, we constructed a biocompatible CS/HA hydrogel, which has similar mechanical properties to native NP tissue. In addition, we have synthesized a KGN-conjugated CS/HA hydrogel and have demonstrated that sustained release of KGN in the hydrogel can promote adipose-derived stem cell (ADSC) proliferation and NP differentiation, and thus enhance the construction of engineered NP tissue.

Materials and methods

Preparation and fabrication of CS/HA hydrogels

For hydrogel preparation, a batch size of 5 mL each was prepared at ambient temperature. A 2% chitosan (CS, deacetylation 90%, Sigma) stock was prepared in 0.1 M hydrochloric acid, and a 10% β-glycerophosphate (GP, Sigma) stock and 1% sodium hyaluronate (HA, 350 kDa, Huaxi Fureida) stock was prepared by dissolving in distilled water. All stock solutions were left at rest at 4 °C overnight to remove bubbles. The 2% CS, 10% GP and 1% HA solutions were subsequently mixed at different proportions (V : V : V, 6 : 3 : 1, 5 : 3 : 2, 4 : 3 : 3, 3 : 3 : 4, 2 : 3 : 5, 1 : 3 : 6) and maintained in a 37 °C water bath prior to use. All percentages in the formulations refer to % (w/v).

Hydrogel characterization

The pH values of the mixtures were measured using a Seven2Go pH-meter with a viscotrode (Mettler Toledo). Three measurements were taken in series on the same sample; four samples in each group were measured.

The interior morphology of the hydrogels was observed using scanning electron microscopy (SEM). Prior to SEM analysis, the samples were dehydrated, dried and gold coated with a sputter coater at 20 mA under 70 mTorr for 1 minute. The surface and cross-sectional morphologies were viewed using a JCM-6000 SEM (JEOL), and pore-size distributions of hydrogels were determined by evaluating a set of at least three SEM images using the linear intercept method.

To observe incorporation of HA in CS hydrogels, the cross-linked CS/HA hydrogels were stained with alcian blue. Briefly, the hydrogels were immersed in 0.5% w/v alcian blue solution dissolved in 10% acetic acid aqueous solution. After staining with gentle shaking for 4 hours, the gels were sequentially washed with 2% acetic acid solution and PBS.

To examine the swelling properties, 1 mL of each hydrogel was weighed before immersing in 5 mL of PBS and maintained at 37 °C for 12 hours. The hydrogels were then removed and immediately weighed with a microbalance after excess water on the surface was absorbed with filter paper. The swelling ratio (SR) was calculated using the following equation: $SR = (W_s - W_d)/W_d$, where W_s and W_d are the weights of the hydrogels at the swelling state and at the dry state, respectively.

To test the mechanical properties, mixtures of the solutions described above were injected into a 96-well culture plate over 15 minutes to obtain columned hydrogels, and these were cut to the same dimensions (~6 mm diameter, ~2 mm height). The Young's modulus was measured in the elastic region of the hydrogels using a Nanotensile testing system (T150 UTM, Agilent) with unconfined compression, up to 20% strain at room temperature. Three measurements were performed per gel and three parallel samples were used.

To examine biodegradability *in vitro*, the hydrogels were incubated in 3 mL of an enzyme solution (100 U mL^{-1} hyaluronidase and 10 mg mL^{-1} lysozyme) in a 37 °C water bath. In brief, hydrogels were pre-weighed (W_0) before quickly freezing at −80 °C and lyophilizing at −50 °C. The weight loss of dry hydrogels was monitored as a function of incubation time in PBS or the enzyme solution at 37 °C. At specified time intervals, hydrogels were quickly frozen at −80 °C, lyophilized and weighed (W_t). The weight loss ratio was calculated as $100\% \times (W_0 - W_t)/W_0$. The weight remaining ratio was defined as $1–100\% \times (W_0 - W_t)/W_0$.

In vitro release study

For preparation of factor-loaded CS/HA hydrogels, KGN was diluted in 10% GP and mixed homogeneously with the CS/HA solution to a final concentration of 50 μM KGN. To examine the release kinetics of KGN from CS/HA hydrogels, each lyophi-

lized KGN-loaded hydrogel was placed in a well of a 24-well microplate and covered with 1 mL PBS. The total volume of PBS was collected and replaced with the same volume of PBS at each sampling time. The amount of KGN released from each CS/HA hydrogel was evaluated using the HPLC (Ultimate 3000, Dionex) spectrum. *In vitro* release was measured in five replicates under physiological conditions (pH 7.3, 37 °C, humidified atmosphere) at different time-points (day 1, 2, 3, 4, 5, 6, 7, 8, 10, 14 and 16).

Cell proliferation and cytotoxicity

GFP-SD rats were purchased from Guangdong Medical Lab Animal Center. Animals were maintained in accordance with the guidelines of the Manipulative Technique for the Care and Use of Laboratory Animals, China, and approved by the Animal Ethical and Welfare Committee of Shenzhen University (SYXK: 2014-0140). ADSC-GFP was isolated from GFP-SD rats with our improved method.[20] ADSCs were cultured and suspended in CS/HA solution at a concentration of 1×10^6 cells per mL. The cross-linked hydrogel was cultured in 1 mL of culture medium (DMEM with 10% FBS) at 37 °C and 5% CO_2 in humidified incubators for 14 days. The viability of encapsulated cells was observed under a SEM, to assess cell distribution and cryosections were stained with hematoxylin and eosin (H&E).

Based on data obtained from preceding experiments, the 5 : 3 : 2 CS/HA hydrogel was chosen for cell proliferation and differentiation. Cell/hydrogel constructs were washed once with PBS and dead cell nuclei were stained with propidium iodide (PI, Invitrogen) at 37 °C for 30 minutes, and observed using a fluorescence microscope (Leica Microsystems). Proliferation of ADSCs in the gels was measured using the cell counting kit (cck-8, Biosource). Cell/hydrogel constructs were washed once with PBS and incubated with cck-8 solution for 3 hours at 37 °C. The cck-8 fluorescence was assayed at 535 nm (excitation) and 600 nm (emission), with four parallel samples being tested.

Differentiation of ADSCs in hydrogels

Four groups were included in the differentiation study; the first group was composed of KGN-loaded hydrogels encapsulating ADSCs that were cultured with differentiation medium (high glucose DMEM supplemented with 10 ng mL^{-1} transforming growth factor-β 3 (TGF-β 3), all from Life Technologies). In the second group, the ADSC encapsulating un-loaded hydrogels were cultured with differentiation medium. The third group was composed of KGN-loaded hydrogels encapsulating ADSCs that were cultured with standard culture medium. The fourth control group with non-loaded hydrogels encapsulating ADSCs was cultured with standard culture medium. ADSCs at passage 5 were encapsulated at a concentration of 1×10^6 cells per mL hydrogel. Each experiment was conducted with three replicates, and culture duration was 28 days. Briefly, pellets of ADSCs were resuspended in 1 mL mixed solution to form the hydrogels. The cell-containing hydrogel solutions were dispensed into 24-well tissue culture plates (1 mL per well) and allowed to form gels at 37 °C. NP differentiation was examined by histological analysis and biochemical quantification.

NP differentiation analysis

For histological analysis, hydrogel samples from the four experimental groups were rinsed with PBS and embedded in the Tissue-Tek® (OCT) compound, snap frozen in liquid nitrogen and stored at −20 °C. Twenty micrometre serial sections from frozen samples were mounted on Superfrost-Plus microscope slides and dried for 24 hours at room temperature. After fixation with methanol/acetone (1 : 1), the cells were rinsed with PBS three times and blocked in 10% normal goat serum for 20 minutes. Samples were incubated with primary antibodies (Anti-Collagen II, Anti-Aggrecan, Abcom) overnight at 4 °C, then rinsed with PBS three times and incubated with horseradish peroxidase (HRP)-conjugated secondary antibodies (Invitrogen) for 2 hours at room temperature. The cells were rinsed with PBS and developed using a DAB kit (Thermo, USA). For semi-quantitative analysis, six pictures for each slide were collected. Image Pro Plus was used to catch the brown area as the area of interest to examine the integrated optical density.

Total RNA from the differentiated cells was obtained using Trizol (Invitrogen). The RNA was reverse transcribed to complementary DNA (cDNA) using the First Strand cDNA kit (Takara) following the manufacturer's protocol. Quantitative polymerase chain reaction (qPCR) analysis was then performed using the Quantitect SYBR Green PCR Master Mix (Takara). Standard curves were generated, and quantities of each transcript were normalized to β-actin as an internal control.

Statistical analysis

Statistical analyses were performed using analysis of variance (ANOVA) followed by the Tukey's *post hoc* test or Student's *t*-test. A value of $P < 0.05$ was considered significant. Results are presented as mean ± standard deviation.

Results

Preparation and characterization of hydrogels

The gelation time of hydrogels was investigated using a vial tilting method (Fig. 1A). The CS/GP/HA solution at 6 : 3 : 1 showed a sol–gel phase transition after 8 minutes at 37 °C. The gelation time increased from 8 to 14 minutes with an increase in the HA concentration. The gelation time of CS/GP/HA hydrogels further increased to 30 minutes as the proportion of the hydrogel changed to 4 : 3 : 3 (Table 1). The addition of HA significantly increased the gelation time, however, the CS/GP/HA solution at 3 : 3 : 4, 2 : 3 : 5 and 1 : 3 : 6 did not change to the gel phase. The pH values of all hydrogel preparations were close to neutral (Table 1).

CS/HA ratios significantly influenced the swelling ratio of hydrogels in PBS. The equilibrium-swelling ratio of CS/HA with 4 : 3 : 3 in PBS was 34%, which was significantly higher than

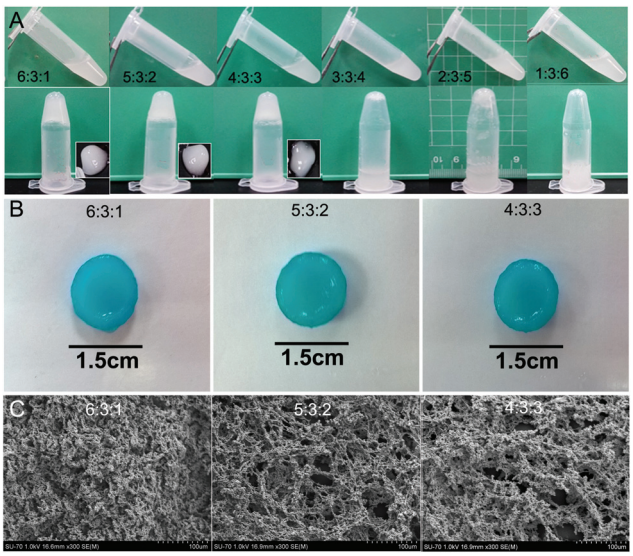

Fig. 1 Fabrication and structure of hydrogels. (A) Images of CS, GP and HA solutions before (sol) and after (gel) incubation at 37 °C. Note that the 3 : 3 : 4, 2 : 3 : 5 and 1 : 3 : 6 mixtures were unable to form gels even after an extended incubation time. (B) Macroscopic images of CS/HA hydrogels stained with alcian blue after incubation in PBS at 37 °C. The diameter of the hydrogels is 1 cm. (C) SEM images of hydrogels. The structure of 4 : 3 : 3 hydrogel is too loose to be broken. Scale bar 100 μm.

the 6 : 3 : 1 hydrogel (Table 1). The equilibrium-swelling ratio increased with the proportion of HA in the hydrogels. The values remained stable up to 7 days in PBS.

The compressive modulus of the hydrogels was determined by a static mechanical analysis method. The 6 : 3 : 1 and 5 : 3 : 2 hydrogels had a significantly higher compressive modulus (2.9 and 1.6 MPa, respectively) than the 4 : 3 : 3 hydrogel (Table 1, $p < 0.05$). The Young's modulus of fresh NP from humans has been reported to be on average 2 MPa, which is close to that of the 5 : 3 : 2 hydrogel. With the incorporation of KGN, the compressive modulus of the composite hydrogels increased, however it was not significantly different from hydrogel only (data not shown).

The CS/HA composite hydrogels without cells were stained with alcian blue to observe HA incorporation and their stability over time (Fig. 1B). The CS/HA hydrogels displayed positive alcian blue staining, indicating the presence of HA in the gels after cross-linking.

The microstructural morphology of dehydrated hydrogels was examined under a SEM (Fig. 1C). Based on the cross-sectional morphology, both hydrogels displayed a continuous and porous structure due to the drying procedure. The pore diameter of the 6 : 3 : 1 CS/HA hydrogel ranged from 10–40 μm, compared to the 5 : 3 : 2 CS/HA hydrogel with pore diameters of 40–80 μm and the 4 : 3 : 3 CS/HA hydrogel with pore diameters ranging from 40–100 μm (Fig. 1C). This difference in the pore size indicates that a higher proportion of CS results in the formation of smaller pore diameters and thus a tighter network structure in thermosensitive hydrogels.

The degradation properties of the composite hydrogels were monitored as a function of incubation time in PBS at 37 °C (Fig. 2A). The ratio of CS/HA had a significant influence on the weight loss behavior of the composite hydrogels. The hydrogels with a higher ratio of CS demonstrated a slower weight loss than the hydrogels with a lower CS composition. Compared with 5 : 3 : 2 and 4 : 3 : 3 hydrogels, the 6 : 3 : 1 hydrogel formed a more compact hydrogel and thus displayed a steady rate of weight loss for up to 14 days and

Table 1 Characteristics of hydrogels prepared with different proportions of CS, GP and HA. n = 5/group, *$p < 0.05$, compared to 6 : 3 : 1

2%CS : 10%GP : 1%HA	Time to gel (min)	PH value	Pore size (μm)	Swelling ratio (%)	Young's modulus (MPa)
6 : 3 : 1	8 ± 0.5	6.8 ± 0.08	10–40	21 ± 2.5	2.9 ± 0.21
5 : 3 : 2	14 ± 0.6	6.92 ± 0.06	40–80	28 ± 3.2	1.6 ± 0.28
4 : 3 : 3	30 ± 0.6	7.03 ± 0.04	40–100	34 ± 3*	0.9 ± 0.18*
3 : 3 : 4	No hydrogel	7.1 ± 0.07	—	—	—
2 : 3 : 5	No hydrogel	7.17 ± 0.1	—	—	—
1 : 3 : 6	No hydrogel	7.21 ± 0.05	—	—	—

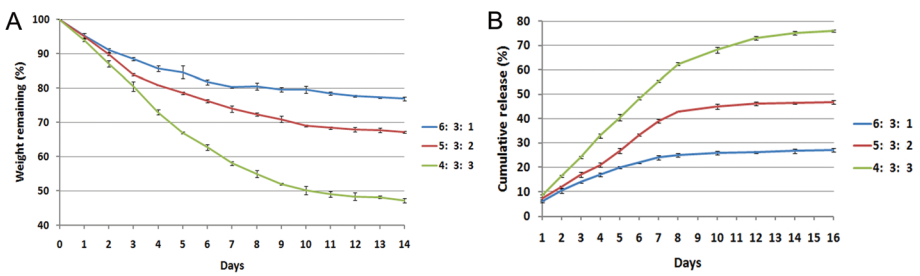

Fig. 2 KGN release profile and degradation properties of hydrogels. (A) *In vitro* degradation of hydrogels after incubation at different time points. Significant mass loss was observed in hydrogels of 4 : 3 : 3. (B) *In vitro* cumulative release profiles of KGN from different hydrogels. Hydrogels with 4 : 3 : 3 showed a quick release of KGN, almost 80% of KGN was released after 2 weeks of incubation.

showed a significantly slower weight loss rate than the other hydrogels. Based on these results, the ratio of 5 : 3 : 2 CS/HA is appropriate for KGN loading and release.

The *in vitro* release of KGN from the hydrogels was determined over 16 days (cumulative release shown in Fig. 2B). The 4 : 3 : 3 CS/HA hydrogels released significantly greater amounts of KGN compared to the 5 : 3 : 2 hydrogels during examination time. In addition, the 6 : 3 : 1 hydrogels displayed slow release of KGN from hydrogels, consistent with their degradation properties. The 5 : 3 : 2 CS/HA hydrogel showed a sustained KGN release over the examination period.

The SEM images of the encapsulated ADSC/hydrogel matrices are presented in Fig. 3A. The residing cells within hydrogels possessed normal spherical or fibroblast-like morphology. CS/HA hydrogels with 5 : 3 : 2 and 4 : 3 : 3 showed more cell survival and bioactivity.

The analysis of the cell-encapsulating hydrogel by H&E staining revealed a relatively uniform distribution of cells throughout the scaffold. CS/HA hydrogels with 5 : 3 : 2 and 4 : 3 : 3 showed more cells than that of 6 : 3 : 1, which was consistent with the observations under a SEM. However, hydrogels with 4 : 3 : 3 were too fragile to handle during examination.

Cell viability and proliferation inside the hydrogel

To assess the suitability of the CS/HA hydrogel to support cell survival, ADSCs were encapsulated in CS/HA hydrogels and cell viability was assessed by propidium iodide (PI) staining of cell-hydrogel constructs over two weeks in culture (Fig. 4B). Most of the cells encapsulated inside CS/HA hydrogels were viable, and maintained a round morphology after one day in culture. CS/HA hydrogels maintained a good overall viability of ADSCs for 14 days in culture, and some cells that were dispersed in the hydrogel showed fibroblast-like morphology (Fig. 4A). After PI staining, the live/dead encapsulated ADSCs within hydrogels after 14 days in culture were imaged by fluorescence microscopy (Fig. 4B). Round or fibroblast-like ADSCs were uniformly distributed in both CS/HA and KGN-conjugated hydrogels. Most of the encapsulated ADSCs survived in copolymer hydrogels after 14 days in culture. Observations using SEM were consistent with the results seen with PI staining (Fig. 5), however, the encapsulation process and two-dimensional culture may still result in cell death. A higher number of live cells were observed in the KGN-conjugated hydrogels than in the pure hydrogels after 14 days of incubation, which was confirmed using the cell proliferation cck-8 assay. In addition, small particles with KGN were observed inside or on the surface of the hydrogels (Fig. 5). Proliferation of encapsulated ADSCs in the CS/HA hydrogel was monitored in culture media at different time-points over 26 days by cck-8 (Fig. 4C). The cells showed significantly higher metabolic activity at days 14–26 compared to days 0–7 ($P < 0.001$), indicating that the cells could grow and proliferate within CS/HA hydrogels.

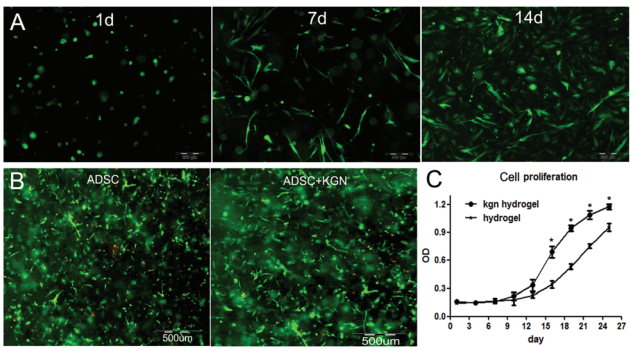

Fig. 4 The effects of KGN on cell viability in hydrogels. (A) Viability of encapsulated ADSCs in CS/HA hydrogels after 1, 7 and 14 days in culture. Scale bar 200 μm. (B) PI fluorescence staining for ADSCs in hydrogels with or without KGN. Scale bar 500 μm. (C) Proliferation assay of ADSCs in hydrogels by CCK-8. ADSC proliferation was significantly enhanced in the presence of KGN, $*p < 0.05$, compare to cells in hydrogels without KGN.

NP differentiation of the encapsulated ADSCs

The NP induced cell-hydrogel constructs were examined by immunohistological methods to identify the distribution of

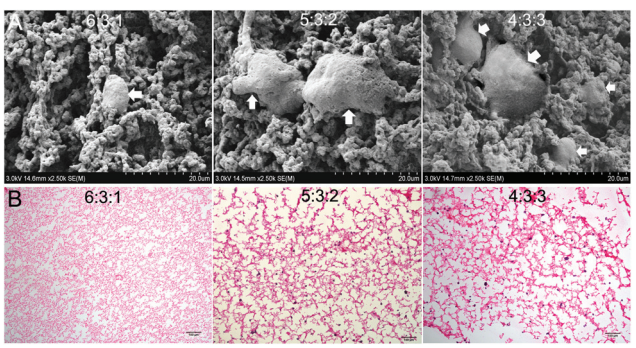

Fig. 3 Morphology of ADSCs in the hydrogels. (A) Scanning electron micrographs of ADSCs in different hydrogels. Cells are indicated with white arrows. Scale bar 20 μm. (B) H&E stained images of encapsulated ADSCs in hydrogels after 14 days in culture. Violet dots indicate the nucleus of ADSCs. Scale bar 100 μm.

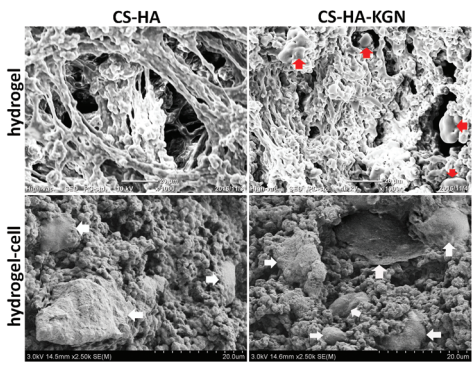

Fig. 5 Scanning electron micrographs of KGN and ADSCs in hydrogels. Small particles can be observed inside or on the surface of hydrogels (red arrow), ADSCs (white arrow) have better viability in hydrogels conjugated with KGN. CS-HA: hydrogel with 5 : 3 : 2, CS-HA-KGN: hydrogel conjugated with KGN. Scale bar 20μm.

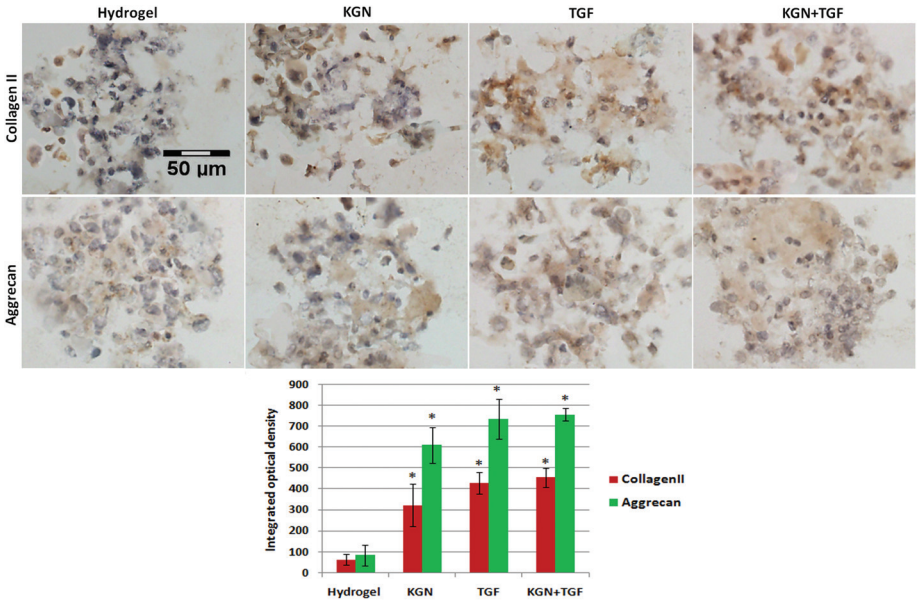

Fig. 6 Expression of collagen II and aggrecan by immunohistochemical staining. Both KGN and TGF-β can promote the differentiation of ADSCs in the hydrogel scaffold to similar extents. Semi-quantitative analysis was done to confirm the results. Scale bar 50 μm.

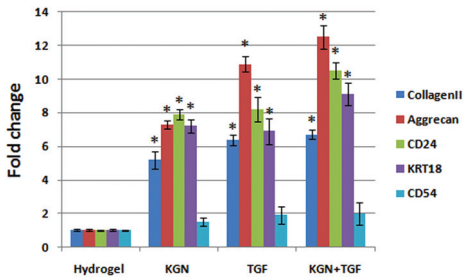

Fig. 7 RT-qPCR for NP genes (collagen II, aggrecan, KRT18, CD24 and CD54) on day 28. Results are shown as fold-change relative to untreated control. *Significant difference compared to the control group.

collagen and aggrecan that are generated. A non-induced construct (control) showed less or minimal staining for collagen II and aggrecan in culture medium at day 28 (Fig. 6). Constructs induced with either KGN or TGF-β expressed collagen II and aggrecan to similar degrees, and induction with both factors together did not further promote the differentiation of ADSCs compared to KGN or TGF-β alone. All the differentiation groups had significantly higher expression of collagen II and aggrecan compared to that of the non-induced groups. The quantitative results from real-time PCR were consistent with the immunohistological staining results (Fig. 7).

Discussion

The cell density within the NP decreases with aging, which results in the loss of proteoglycan synthesis and a decline in the production of important ECM proteins such as aggrecans and type II collagen.[21] Chitosan is structurally analogous to GAGs, and HA is a major component of the ECM in the NP.[10,12,14] Hydroxyl groups in HA can cross-link with amino groups in CS. CS when combined with glycerol phosphate and HA can undergo a sol–gel transition at 37 °C by covalent cross-linking.[22] We have shown in this study that increasing the HA concentration in the CS/HA thermo-sensitive hydrogel increases the gelation time, which may be attributable to the presence of more hydrophilic groups among HA chains.

In addition to gel thermosensitivity, other important requirements include high water content, biodegradability as well as mechanical properties,[23] which are important to the mechanical function of the disc after implantation, and it is important that the matrix secreted from implanted cells is able to replace the hydrogel over time after the implantation. The hydrogels with a higher HA content displayed a loose structure, consequently increasing the exposure of hydrophilic polymer chains to water molecules at 37 °C, leading to enhanced water absorption and significantly faster weight loss. This is likely due to the complicated entanglement of macromolecular chains,[5] and accordingly, a higher ratio of CS resulted in a tighter network structure and a smaller pore diameter in the hydrogels.

We chose the hydrogel that demonstrated similar mechanical properties to native NP tissue. Since the microstructure, mechanical properties and high water content of 5 : 3 : 2 hydrogels are very similar to those of the extracellular matrix of natural NP tissue, these hydrogels may provide an environment for maintaining cell bioactivity and preserving the cell phenotype. We used ADSCs for the regeneration of engineered NP tissue, because they can be easily obtained from autologous adipose tissue, and we have demonstrated that their pro-

liferation and differentiation ability are much stronger than that of bone marrow derived stem cells. These cells have been widely investigated for use in cartilage and other tissue regeneration.[24–26] ADSCs showed good morphology and strong proliferation ability in CS/HA hydrogels. Incorporation of ADSCs into the CS/HA hydrogel may aid ADSC proliferation and NP differentiation since native NP cells prefer to live in a three dimensional microenvironment. This also enables mechanical load transduction, which is important for the synthesis of the NP matrix.[27] Incorporating cells into the CS/HA hydrogel solution reduces clustering and poor distribution of transplanted cells. Moreover, after gelation, the hydrogel provides a temporary three-dimensional matrix to increase cell retention and survival.

The CS/HA hydrogel can also create a favorable NP-like microenvironment due to the incorporation of ECM components present in NP tissue.[28–32] The presence of CS, which is analogous to GAGs and the ECM component HA may support the growth and deposition of cells, which may play a special role in modulating NP differentiation and function.[6,13]

CS/HA hydrogels can also serve as a delivery device not only for mobilizing stem cells to the injection site, but also for sustainable release of bioactive molecules or growth factors. KGN is a recently characterized molecule that promotes the differentiation of stem cells into chondrocytes for cartilage regeneration. KGN is a low molecular weight and hydrophobic compound, in which the amino groups of chitosan can couple covalently to its carboxyl groups.[18] We conjugated KGN into the CS/HA hydrogel to enhance the aqueous solubility and sustained release from the hydrogel. Similar to previous studies,[18] the conjugation of KGN to the hydrogel enhanced the proliferation and differentiation of NP cells. During differentiation of stem cells, KGN frees core-binding factor (CBF)-b, which may bind to the DNA-binding transcription factor RUNX1 to activate the transcription of collagen II and aggrecan.[17] In addition, KGN has similar ability to induce differentiation to TGF-β, but cannot further promote or enhance the effect of TGF-β, therefore is a suitable replacement of TGF-β for NP and cartilage differentiation and regeneration. After construction of NP-like tissues, the next step is implantation. As we all know, the inflammation environment is one of the key factors for DDD, CD54 can be used as a biomarker to evaluate the inflammation-associated disc degeneration, because the expression of CD54 was insignificant in younger NP tissue, and showed stronger expression in aged NP tissue.[33] There is no significant increase of CD54 expression after differentiation in the hydrogel, which indicated that there is no inflammation reaction occurring in our constructed hydrogel, and will cause no harm to native disc after implantation.

Conclusions

In our study, chitosan was chosen to mimic the GAG structure in the NP ECM, and HA as a major component of NP ECM, to construct a CS/HA injectable hydrogel that can support proliferation of ADSCs and promote differentiation towards NP-like tissues. In addition, a KGN-conjugated hydrogel has the potential to support ADSC distribution and related factor delivery, which significantly promotes NP cell differentiation in hydrogels and development of engineered NP tissues. Thus, this type of hydrogel with encapsulated ADSCs and KGN may fill damaged NP defects and can be applied during minimally invasive surgery. However, further work is needed to understand the mechanism of how the CS/HA hydrogel affects the production of type II collagen and aggrecan by ADSCs, and animal studies will be needed to investigate the efficacy of NP regeneration of the CS/HA hydrogel–ADSC system.

Acknowledgements

This work was supported by National Natural Science Foundation of China (No. 81301597) and the Shenzhen Special funds for the Emerging Strategic Industry Development (No. JCYJ20150525092940984, JCYJ20150525092940973, JCYJ20160422090807181).

Notes and references

1 D. S. Mern, A. Beierfuß, C. Thomé and A. A. Hegewald, *J. Tissue Eng. Regener. Med.*, 2014, **8**, 925–936.
2 D. Drazin, J. Rosner, P. Avalos and F. Acosta, *Adv. Orthop.*, 2012, **2012**, 1–8.
3 D. Oehme, T. Goldschlager, J. V. Rosenfeld, P. Ghosh and G. Jenkin, *Neurosurg. Rev.*, 2015, **38**, 429–445.
4 S. H. Söntjens, D. L. Nettles, M. A. Carnahan, L. A. Setton and M. W. Grinstaff, *Biomacromolecules*, 2006, **7**, 310–316.
5 H. Tan, J. P. Rubin and K. G. Marra, *Organogenesis*, 2010, **6**, 173–180.
6 M. B. Nair, G. Baranwal, P. Vijayan, K. S. Keyan and R. Jayakumar, *Colloids Surf., B*, 2015, **136**, 84–92.
7 Y. P. Singh, N. Bhardwaj and B. B. Mandal, *ACS Appl. Mater. Interfaces*, 2016, **8**, 21236–21249.
8 S. Atta, S. Khaliq, A. Islam, I. Javeria, T. Jamil, M. M. Athar, M. I. Shafiq and A. Ghaffar, *Int. J. Biol. Macromol.*, 2015, **80**, 240–245.
9 S. Ravindran, Q. Gao, M. Kotecha, R. L. Magin, S. Karol, A. Bedran-Russo and A. George, *Tissue Eng., Part A*, 2012, **18**, 295–309.
10 H. Tan, C. M. Ramirez, N. Miljkovic, H. Li, J. P. Rubin and K. G. Marra, *Biomaterials*, 2009, **30**, 6844–6853.
11 F. Wang and X. He, *Exp. Ther. Med.*, 2015, **9**, 493–500.
12 C. W. Ha, Y. B. Park, J. Y. Chung and Y. G. Park, *Stem Cells Transl. Med.*, 2015, **4**, 1044–1051.
13 D. H. Kim, J. T. Martin, D. M. Elliott, L. J. Smith and R. L. Mauck, *Acta Biomater.*, 2015, **12**, 21–29.
14 H. Naderi-Meshkin, K. Andreas, M. M. Matin, M. Sittinger, H. R. Bidkhori, N. Ahmadiankia, A. R. Bahrami and J. Ringe, *Cell Biol. Int.*, 2014, **38**, 72–84.

15 Y. Shi, Z. Xiong, X. Lu, X. Yan, X. Cai and W. Xue, *J. Mater. Sci. Mater. Med.*, 2016, **27**, 169.
16 Z. Karimi, M. Ghorbani, B. Hashemibeni and H. Bahramian, *Adv. Biomed. Res.*, 2015, **4**, 251.
17 K. Johnson, S. Zhu, M. S. Tremblay, J. N. Payette, J. Wang, L. C. Bouchez, S. Meeusen, A. Althage, C. Y. Cho, X. Wu and P. G. Schultz, *Science*, 2012, **336**, 717–721.
18 M. L. Kang, J. Y. Ko, J. E. Kim and G. I. Im, *Biomaterials*, 2014, **35**, 9984–9994.
19 Y. Ono, S. Ishizuka, C. B. Knudson and W. Knudson, *Cartilage*, 2014, **5**, 172–180.
20 Y. Zhu, T. Liu, K. Song, R. Ning, X. Ma and Z. Cui, *Mol. Cell. Biochem.*, 2009, **324**, 117–129.
21 C. K. Kepler, D. G. Anderson, C. Tannoury and R. K. Ponnappan, *J. Am. Acad. Orthop. Surg.*, 2011, **19**, 543–553.
22 S. Kaderli, C. Boulocher, E. Pillet, D. Watrelot-Virieux, A. L. Rougemont, T. Roger, E. Viguier, R. Gurny, L. Scapozza and O. Jordan, *Int. J. Pharm.*, 2015, **483**, 158–168.
23 S. Xue, D. Pei, W. Jiang, Y. Mu and X. Wan, *Polymer*, 2016, **99**, 340–348.
24 Y. Zhu, T. Liu, K. Song, X. Fan, X. Ma and Z. Cui, *Cell Biochem. Funct.*, 2008, **26**, 664–675.
25 Y. Zhu, T. Liu, H. Ye, K. Song, X. Ma and Z. Cui, *Stem Cells Dev.*, 2010, **19**, 1547–1556.
26 R. Kasir, V. N. Vernekar and C. T. Laurencin, *Regen. Eng. Transl. Med.*, 2015, **1**, 42–49.
27 A. T. Francisco, R. J. Mancino, R. D. Bowles, J. M. Brunger, D. M. Tainter, Y. T. Chen, W. J. Richardson, F. Guilak and L. A. Setton, *Biomaterials*, 2013, **34**, 7381–7388.
28 H. Park, B. Choi, J. Hu and M. Lee, *Acta Biomater.*, 2013, **9**, 4779–4786.
29 C. R. Correia, L. S. Moreira-Teixeira, L. Moroni, R. L. Reis, C. A. van Blitterswijk, M. Karperien, *et al.*, *Tissue Eng., Part C*, 2011, **17**, 717–730.
30 K. L. Spiller, S. A. Maher and A. M. Lowman, *Tissue Eng., Part B*, 2011, **17**, 281–299.
31 Y. C. Huang, V. Y. Leung, W. W. Lu and K. D. Luk, *Spine J.*, 2013, **13**, 352–362.
32 Y. C. Huang, J. P. Urban and K. D. Luk, *Nat. Rev. Rheumatol.*, 2014, **10**, 561–566.
33 X. Tang, L. Jing, W. J. Richardson, R. E. Isaacs, R. D. Fitch, C. R. Brown, M. M. Erickson, L. A. Setton and J. Chen, Identifying molecular phenotype of nucleus pulposus cells in human intervertebral disc with aging and degeneration, *J. Orthop. Res.*, 2016, **34**, 1316–1326.